

MUSE-adaptive optics view of the starburst-AGN connection: NGC 7130

Johan H. Knapen^{1,2}, Sébastien Comerón³ and Marja K. Seidel⁴

¹Instituto de Astrofísica de Canarias, E-38205 La Laguna, Tenerife, Spain

²Departamento de Astrofísica, Universidad de La Laguna, E-38205 La Laguna, Tenerife, Spain

³University of Oulu, Astronomy Research Unit, P.O. Box 3000, FI-90014 Oulu, Finland

⁴Caltech-IPAC, MC 314-6, 1200 E California Blvd, Pasadena, CA 91125, USA

Abstract. We combine ALMA and MUSE-NFM (narrow field mode, with full four-laser adaptive optics correction) data at 0.15 arcsec spatial resolution of the archetypical AGN-starburst “composite” galaxy NGC 7130. We present the discovery of a small 0.''2 (60 pc) radius kinematically decoupled core or small bi-polar outflow, as well as a larger-scale outflow. We confirm the existence of star-forming knots arranged in an 0.''58 (185 pc) radius ring around the Seyfert 1.9 nucleus, previously observed from UV and optical *Hubble Space Telescope* and CO(6-5) ALMA imaging. An extinction map derived from the MUSE data highlights the regions of enhanced CO emission as clearly seen in the ALMA data. We determine the position of the nucleus as the location of a peak in gas velocity dispersion. A plume of material extends towards the NE from the nucleus until at least the edge of our field of view at 2'' (640 pc) radius which we interpret as an outflow originating in the AGN. The plume is not visible morphologically, but is clearly characterised in our data by emission lines ratios characteristic of AGN emission, enhanced gas velocity dispersion, and distinct non-circular gas velocities. Its orientation is roughly perpendicular to the line of nodes of the rotating host galaxy disk. An 0.''2-radius circumnuclear area of positive and negative velocities indicates a tiny inner disk or a small bipolar outflow, only observable when combining the integral field spectroscopic capabilities of MUSE with full adaptive optics.

Keywords. Galaxies: active – Galaxies: individual: NGC 7130 – Galaxies: ISM – Galaxies: outflows – Galaxies: nuclei – Galaxies: Seyfert

1. Introduction

Accretion onto a supermassive black hole, in combination with increased cold gas availability due to inflow, may simultaneously increase the star formation (SF) and the active galactic nucleus (AGN) activity in the centre of a galaxy.

Inflowing gas must lose by far most of its angular momentum before it reaches the very central regions (e.g., [Begelman *et al.* 1984](#); [Shlosman *et al.* 1989](#)), but can do so under the influence of non-axisymmetries in the host galaxy induced by bars or past or present interactions. The resulting availability of gaseous fuel can lead to both starburst and AGN activity, which can even occur simultaneously and which is then referred to as “composite”. Studying the gas physics, stellar properties, and kinematics of composite AGN/starburst galaxies is important as it provides direct links to the physics of the gas transport and the activity, star-forming and/or AGN, that may result.

We study one of the best-known examples of such composite AGN-starburst galaxies: the luminous infrared galaxy NGC 7130 (also known as IC 5135), a peculiar Sa ([de Vaucouleurs *et al.* 1991](#)) galaxy at a distance of 65.5 Mpc (so 1'' corresponds to 318 pc). NGC 7130 hosts a Seyfert 1.9 AGN nucleus ([Véron-Cetty & Véron 2006](#)) as well as a powerful compact circumnuclear starburst ([Phillips *et al.* 1983](#)). We study this

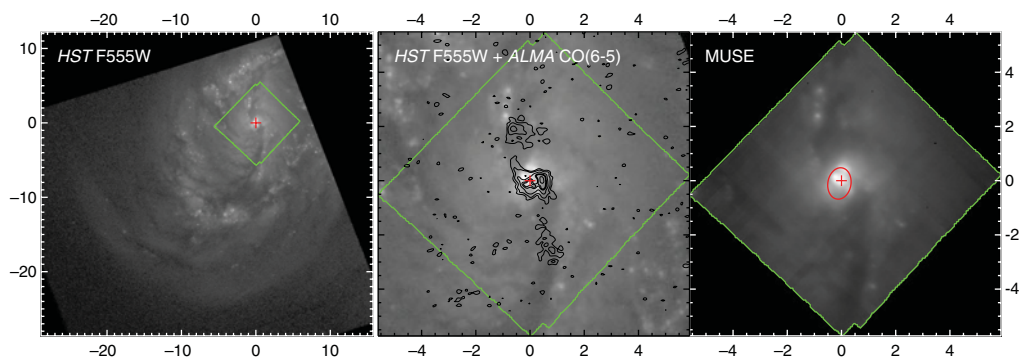


Figure 1. *Left:* *HST* image of NGC 7130 in the F555W band. The red + sign indicates the centre of the galaxy and the green contour indicates the MUSE field of view. *Middle:* enlarged version of the image on the *left*. The black contours indicate the CO(6-5) intensity as observed by ALMA. *Right:* white-light image obtained by collapsing the MUSE datacube along its wavelength axis. The red ellipse indicates the outline of the circumnuclear ring. The angular resolution achieved by MUSE + AO is similar to that of the *HST*. Axis labels in arcsec, N is up and E to the right.

galaxy with new integral field spectroscopy obtained with MUSE-NFM (narrow field mode) on the ESO-VLT, which uses the adaptive optics (AO) system GALACSI with four laser guide stars to feed MUSE. Further details are given in Knapen *et al.* (2019, KCS19 hereinafter) and in Comerón, Knapen & Seidel (2020, in prep).

2. Observations

We used the MUSE integral field spectrograph on the VLT in its NFM in conjunction with the AO system GALACSI during September 2018. In addition to GALACSI's four laser guide stars, we used the Seyfert nucleus of NGC 7130 as a natural guide star. The resulting field of view (FOV) is $7''.59 \times 7''.59$ with a sampling of $0''.0253$ per pixel, and the resulting spatial resolution achieved was $0''.15 - 0''.18$, obtained on Sept 18. The resulting data were reduced using v. 2.5.2 of the MUSE pipeline (Weilbacher *et al.* 2012) and additional software; details have been described in KCS19. We fitted the stellar component in the spectra using pPXF (Cappellari, & Emsellem 2004; Cappellari 2017). In addition, we used an archival WFPC3 F555W *HST* image, 600 s deep (six different exposures) and with $\sim 0''.1$ angular resolution, and the ALMA CO(6-5) data with a resolution of $0''.20 \times 0''.14$ from Zhao *et al.* (2016).

3. Results

Figure 1 shows how the optical image reconstructed from the MUSE data cube has excellent spatial resolution—comparable to that of the *HST* image. We also show the CO emission as observed with ALMA, outlining spiral-shaped regions of enhanced gas and thus dust obscuration.

The MUSE spectral data allow us to fit many different absorption and emission lines. We concentrate here on gas emission lines, which we showed in KCS19 to offer evidence for an outflow region to the NW of the (AGN) nucleus, clearly offset from the rest of the inner region by AGN-like emission line ratios, enhanced velocity dispersion, and deviant gas velocities.

We now take the next step in our analysis, which is to fit two components to the gas emission ($H\beta$, [OIII] $\lambda 4959$, [OIII] $\lambda 5007$, [NI] $\lambda 5198$, [NI] $\lambda 5200$, [OI] $\lambda 6300$, [OI] $\lambda 6364$, [NII] $\lambda 6548$, $H\alpha$, [NII] $\lambda 6583$, [SII] $\lambda 6716$, and [SII] $\lambda 6731$ lines). The resulting velocity and

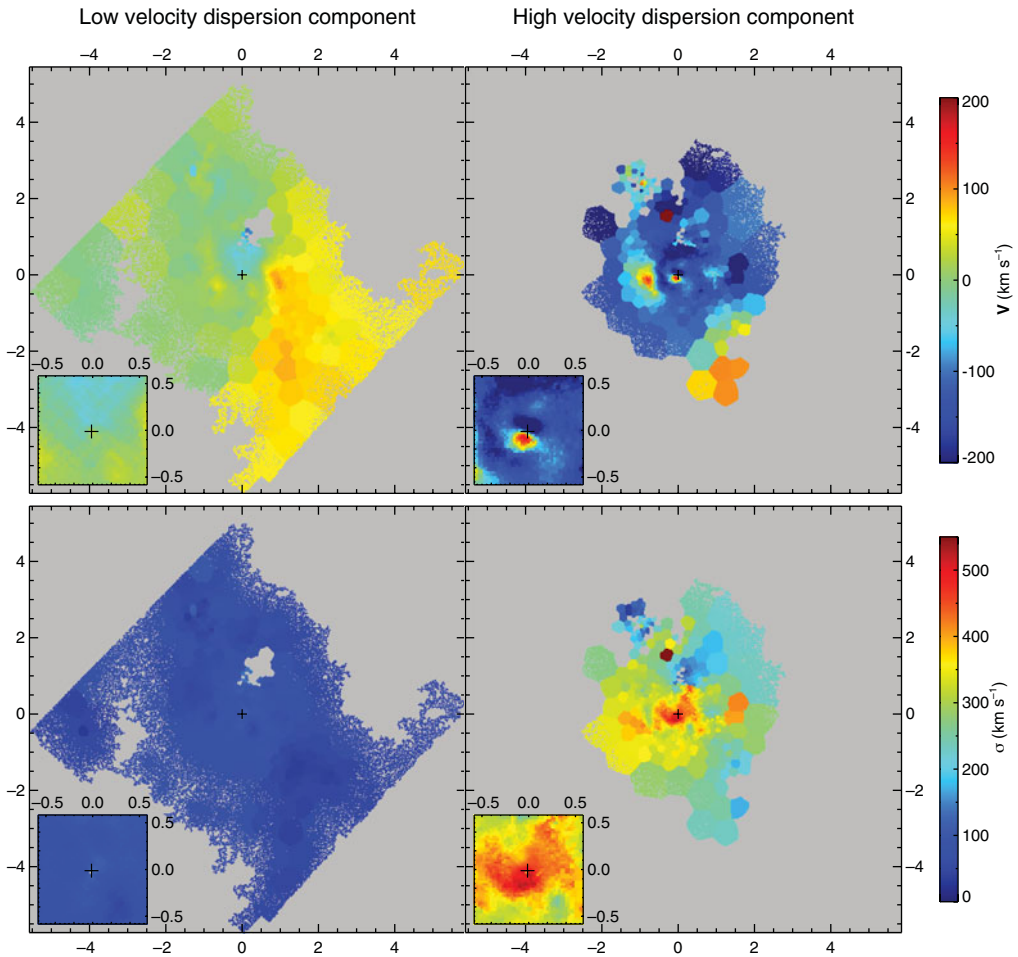


Figure 2. Velocity (V ; *upper panels*) and velocity dispersion (σ ; *lower panels*) maps for the low-velocity dispersion (cold, *left column*) and the high-velocity dispersion (hot, *right column*) components of the ionised gas in NGC 7130. An enlarged view of the central arcsecond is presented in the insets. The cold component shows rotation and can be associated with the disc of the galaxy. The hot component has typical velocities of up to 200 km s^{-1} with respect to the galaxy disc and can be associated with an outflow. The innermost region of the high-velocity dispersion component shows a tiny structure, $0''.2$ in radius, that can be interpreted as either a nuclear disc or a bipolar outflow. Axis labels in arcsec, N is up and E to the right.

velocity dispersion fields are shown in Fig. 2, separately for the low- (left panels) and high-velocity dispersion (right) components of the gas. We see that the low-velocity component cleanly separates and outlines a rotating disk. The high-velocity dispersion component, in contrast, traces non-rotating structure in the velocity field, whereas the dispersions correlate with the outline of the AGN-related outflow identified in KCS19. KCS19 also identified a small kinematically decoupled core, of around $0''.2$ or 60 pc in radius. From Fig. 2 we now see that this core is only visible in the high-dispersion maps, which is strong evidence in favour of it being connected to, or even part of, the AGN-driven gas outflow.

Figure 3 highlights the different emission line ratios in the low- and high-velocity dispersions as defined above. We show the so-called BPT (after Baldwin, Phillips &

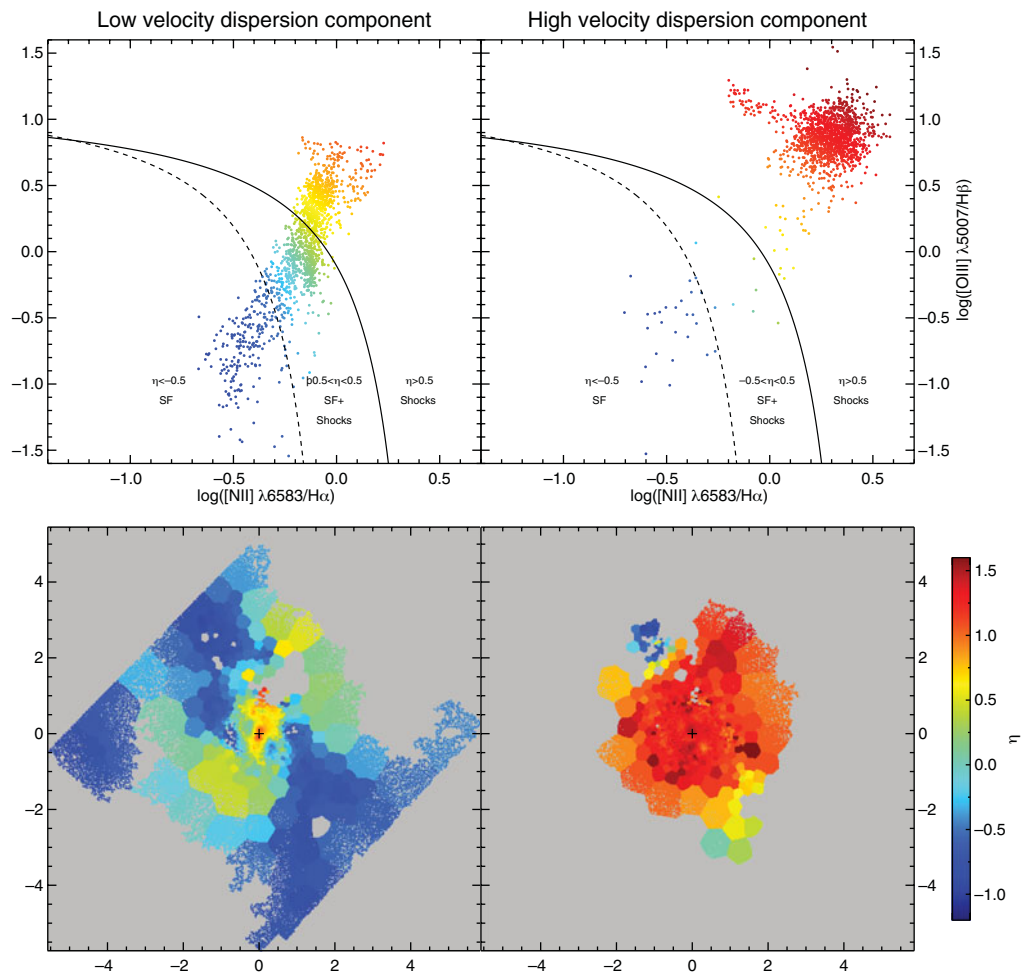


Figure 3. For the low-velocity dispersion component (*left*) and the high-velocity dispersion component (*right*), we show in the *upper* panels: the $[\text{O III}]/\text{H}\beta$ vs $[\text{N II}]/\text{H}\alpha$ diagnostic diagram used to build the BPT maps, and in the *lower* panels: resolved BPT diagrams. Each of the data points corresponds to one of the bins in the *upper* row. The points and the bins are colour-coded according to their η , a parameter that describes the distance between a given point in the diagnostic diagram and the bisector line between the continuous and the dashed lines in the plot (Erroz-Ferrer *et al.* 2019). Blue points indicate regions ionised by star formation whereas red points indicate shock ionisation. The disc of the galaxy (low-velocity dispersion component) is mostly ionised by star formation. The outflow is clearly shock-ionised. Axis labels in arcsec, N is up and E to the right.

Terlevich 1981) line ratio diagnostic diagrams for these two components separately, the low-dispersion component again on the left (upper panels). The points in the BPT diagrams are colour-coded by how far from the central lines they are, and are then mapped, with these colours, back into the spatial plane (lower panels). We see that the disc of the galaxy is mostly blue, which indicates star formation, whereas the high-velocity dispersion component returns almost exclusively red colours, which is shocked gas. This confirms that the high-dispersion component is driven by shocks, most likely by the AGN. The outflow zone is indeed seen to be related to both high dispersion and a shocked origin of the emission line ratios, confirming what we described in KCS19.

4. Conclusions

We present new adaptive optics MUSE integral-field observations, combined with archival *HST* and ALMA imaging, of the archetypical AGN-starburst composite galaxy and Seyfert 2 host NGC 7130. We reach *HST*-like spatial resolution, but with the full complement of absorption and emission lines of MUSE at our disposal. We find an outflow region of at least ~ 600 pc, presumably driven by the AGN, which is set apart from the rest of the inner region by enhanced gas velocity dispersion, non-circular velocities, and emission line ratios indicative of shocks (see KCS19 for details).

We separate two components of the gas emission, with low and high velocity dispersion, and plot the velocity and dispersion fields as well as BPT diagnostic diagrams separately for these two components. The low-dispersion gas traces the star-forming and rotating inner disk of the galaxy. The high-dispersion component, in contrast, highlights the outflow region and shows the extent to which part of the gas across the inner kpc region is shocked, presumably by the AGN. A small kinematically decoupled core, see in KCS19, manifests itself exclusively in the high-dispersion gas, which is evidence for it being connected to the AGN and/or the outflow, rather than it being a traditional small disk rotating in a different plane.

Acknowledgements

J.H.K. acknowledges financial support from the European Union's Horizon 2020 research and innovation programme under Marie Skłodowska-Curie grant agreement No 721463 to the SUNDIAL ITN network, from the State Research Agency (AEI) of the Spanish Ministry of Science, Innovation and Universities (MCIU) and the European Regional Development Fund (FEDER) under the grant with reference AYA2016-76219-P, from IAC project P/300724, financed by the Ministry of Science, Innovation and Universities, through the State Budget and by the Canary Islands Department of Economy, Knowledge and Employment, through the Regional Budget of the Autonomous Community, and from the Fundación BBVA under its 2017 programme of assistance to scientific research groups, for the project "Using machine-learning techniques to drag galaxies from the noise in deep imaging".

References

- Baldwin, J. A., Phillips, M. M., & Terlevich, R. 1981, *PASP*, 93, 5
- Begelman, M. C., Blandford, R. D., & Rees, M. J. 1984, *Rev. Mod. Phys.*, 56, 255
- Cappellari, M. 2017, *MNRAS*, 466, 798
- Cappellari, M. & Emsellem, E. 2004, *PASP*, 116, 138
- de Vaucouleurs, G., de Vaucouleurs, A., Corwin, Jr., H. G., *et al.* 1991, Third Reference Catalogue of Bright Galaxies
- Erroz-Ferrer, S., Carollo, M. C., den Brok, M., *et al.* 2019, *MNRAS*, 484, 5009
- Knapen, J. H., Comerón, S., & Seidel, M. K. 2019, *A&A*, 621, L5 (KCS19)
- Phillips, M. M., Charles, P. A., & Baldwin, J. A. 1983, *ApJ*, 266, 485
- Shlosman, I., Frank, J., & Begelman, M. C. 1989, *Nature*, 338, 451111
- Véron-Cetty, M. P. & Véron, P. 2006, *A&A*, 455, 773
- Weilbacher, P. M., Streicher, O., Urrutia, T., *et al.* 2012, *SPIE*, 8451, 84510B
- Zhao, Y., Lu, N., Xu, C. K., *et al.* 2016, *ApJ*, 820, 118